

Electronic Supporting Information for:

**Consistent supramolecular assembly arising from
a mixture of components – self-sorting and solid solutions
of chiral oxygenated trianglimines**

Joanna Szymkowiak, Beata Warżajtis, Urszula Rychlewska, and Marcin Kwit,

Table of contents

Experimental details	S13
Calculations details	S18
Comments regarding plausible mechanism of trianglimine 9 formation	S18
Details of SCXRD measurements	S18
Tables S1-S7	S110
Figures S1-S9	S118
References	S131

Experimental details

All commercially available reagents were obtained from commercial suppliers and used for reactions without further purification, unless specified otherwise. The anhydrous dichloromethane and chloroform were distilled over calcium hydride under inert atmosphere and kept under argon atmosphere. Flash column chromatography was performed on Merck Kieselgel type 60 (250-400 mesh). Merck Kieselgel type 60F₂₅₄ analytical plates were used for TLC.

¹H and ¹³C NMR spectra were recorded on a Bruker Advance III 600MHz, Bruker 400 MHz or Bruker 300 MHz at ambient temperature. The ¹H NMR spectra are reported in parts per million (ppm) downfield of TMS and were measured relative to the signals for CDCl₃ or DMSO-*d*₆. The ¹³C NMR spectra were reported in ppm relative to residual CDCl₃ or DMSO-*d*₆ signals and were obtained with ¹H decoupling. Mass spectra were recorded on AB Sciex TripleTOF® 5600+ System and *Bruker UltrafleXtreme* MALDI-TOF/TOF spectrometer with DHB matrix. Melting points were measured using open glass capillaries in a Büchi Melting Point B-545 apparatus. A Jasco P-2000 polarimeter was used for optical rotation measurements (at 20 °C). FT-IR spectra were measured in KBr pellets using Jasco 4000 FTIR spectrometer or at ATR equipment using Thermo Scientific Nicolet iS50 FTIR spectrometer and are reported as wave numbers in cm⁻¹.

All known compounds were identified by spectroscopic comparison with authentic samples.

2-Hydroxyterephthalaldehyde 4.

To a stirred solution of 2-methoxyterephthalaldehyde (**5**, 0.82 g, 5 mmol) in dry dichloromethane (100 mL) under argon atmosphere was added drop wise BBr₃ (10 mL, 10 mmol, 1M solution in CH₂Cl₂), and the solution was stirred for 4h at room temperature. After that time the reaction mixture was neutralized by careful addition of saturated NaHCO₃ solution, then transferred into the separatory funnel and extracted several times with dichloromethane. The combined organic extracts were washed with brine, dried over anhydrous Na₂SO₄ and concentrated under vacuum. The crude product was purified by column chromatography on silica gel using heptane - dichloromethane (1:1) as eluent to give pure white solid (200 mg, 27% yield).

m.p. 101 - 102 °C;

¹H NMR (300 MHz, CDCl₃): δ = 11.03 (s, 1H), 10.05 (s, 1H), 10.03 (s, 1H), 7.76 (d, *J* = 7.9 Hz, 1H), 7.54 (dd, *J* = 7.9, 1.4 Hz, 1H), 7.48 (m, 1H);

¹³C NMR (400 MHz, CDCl₃): δ = 196.58, 191.20, 161.87, 141.86, 134.40, 123.66, 119.53, 119.49;

MS (HR ESI-TOF): *m/z* found 149.0249 [M-H]⁻, calcd for C₈H₅O₃ 149.0239;

IR (ATR): $\tilde{\nu}$ = 3190, 3059, 2863, 1693, 1653, 1570, 1498, 1446, 1356, 1276, 1219, 1188, 1150, 967, 778, 665 cm⁻¹.

2-Methoxyterephthalaldehyde 5

The title compound was obtained according to the previously published procedure.[1]

m.p. 102 - 103 °C;

¹H NMR (300 MHz, CDCl₃): δ = 10.54 (s, 1H), 10.06 (s, 1H), 8.00 (d, *J* = 7.84 Hz, 1H), 7.53 (m, 2H), 4.03 (s, 3H);

¹³C NMR (300 MHz, CDCl₃): δ = 191.49, 189.34, 161.90, 141.35, 129.22, 128.62, 123.17, 110.70, 56.06;

IR (KBr): $\tilde{\nu}$ = 2860, 1681, 1575, 1491, 1471, 1424, 1390, 1311, 1263, 1184, 1150, 1027, 826, 814, 743 cm⁻¹.

2,5-Dihydroxyterephthalaldehyde 6

The title compound was obtained according to the modified procedure previously proposed by Okada *et al.*[2] To a stirred solution of 2,5-dimethoxyterephthalaldehyde (**7**, 0.5 g, 2.6 mmol) in dry dichloromethane (100 mL), under argon atmosphere, BBr₃ was added drop wise (15 mL, 15 mmol, 1M solution in CH₂Cl₂), and the solution was stirred for 4h at room temperature. Then the reaction mixture was neutralized by addition of saturated NaHCO₃ solution, transferred into the separatory funnel and extracted several times with dichloromethane. The combined organic extracts were washed with brine, dried over anhydrous Na₂SO₄ and concentrated under reduced pressure. The crude product was recrystallized from acetone - chloroform mixture of solvents to provide a yellow crystal product (300 mg, 70% yield).

m.p. 169 °C;

¹H NMR (300 MHz, CDCl₃): δ = 10.23 (s, 2H), 9.96 (s, 2H), 7.24 (s, 2H);

¹³C NMR (300 MHz, CDCl₃): δ = 196.42, 153.26, 125.19, 121.61;

IR (ATR): $\tilde{\nu}$ = 3487, 3264, 3053, 2890, 1663, 1475, 1459, 1277, 1122, 888, 832, 792, 665, 507 cm⁻¹.

2,5-Dimethoxyterephthalaldehyde 7

Aldehyde **7** was obtained according to the published procedure.[3]

m.p. 214 °C;

¹H NMR (300 MHz, CDCl₃): δ = 10.50 (s, 1H), 7.50 (s, 1H), 3.95 (s, 3H);

¹³C NMR (300 MHz, CDCl₃): δ = 189.24, 155.73, 129.13, 110.90, 56.22;

IR (ATR): $\tilde{\nu}$ = 3336, 3052, 2990, 2955, 2870, 2761, 1668, 1480, 1393, 1301, 1210, 1127, 1017, 876, 657 cm⁻¹.

Trianglimine 8

The title compound was obtained according to the previously published procedure.[4]

m.p. does not melt up to 360 °C;

¹H NMR (300 MHz, CDCl₃): δ = 8.14 (s, 1H), 7.52 (s, 2H), 3.36 (m, 1H), 1.82 (m, 3H), 1.47 (m, 1H);

¹³C NMR (400 MHz, CDCl₃): δ = 160.17, 137.69, 127.97, 74.36, 32.69, 24.42;

MS (HR ESI-TOF⁺): m/z found 637.4027 [M+H]⁺, calcd C₄₂H₄₉N₆ 637.4019;

[α]_D²⁰ -317.4 (c = 1, CHCl₃);

IR (ATR): $\tilde{\nu}$ = 2925, 2854, 1639, 1448, 1416, 1373, 1342, 1298, 1218, 1084, 932, 855, 822 cm⁻¹.

Trianglimine 9

The title compound was obtained according to the previously published procedure.[5]

m.p. decomposed above 250 °C;

¹H NMR (600 MHz, CDCl₃): δ = 13.36 (br, 1H), 13.18 (br, 0.5H), 8.21 (s, 1H), 8.19 (m, 0.5H), 8.08 (d, J = 4.75 Hz, 0.5H), 8.06 (s, 1H), 7.32 (m, 0.5H), 7.28 (m, 1H), 7.06 (m, 1.5H), 6.80 (m, 1.5H), 3.38 (m, 1.5H), 3.26 (m, 1.5H), 1.73 (m, 5H), 1.46 (m, 3H), 1.25 (m, 1H);

¹³C NMR (600 MHz, CDCl₃): δ = 164.34, 164.18, 164.02, 163.89, 161.32, 161.23, 161.01, 160.93, 160.68, 160.43, 160.26, 160.06, 139.42, 139.22, 139.09, 138.91, 131.68, 131.62, 131.32, 131.21, 119.78, 119.76, 119.63, 119.53, 119.37, 119.16, 115.70, 115.45, 115.35, 115.12, 74.70, 74.63, 74.55, 73.44, 73.32, 73.11, 73.01, 33.00, 32.96, 32.87, 32.82, 32.75, 32.72, 32.69, 32.66, 24.42, 24.38, 24.29, 24.24, 24.23;

MS (HR ESI-TOF⁺): m/z found 685.3861 [M+H]⁺, calcd C₄₂H₄₉N₆O₃ 685.3866;

[α]_D²⁰ -546.4 (c = 1, CHCl₃);

IR (ATR): $\tilde{\nu}$ = 2926, 2855, 2659, 1623, 1566, 1512, 1447, 1367, 1342, 1291, 1211, 1165, 1140, 1090, 1038, 973, 935, 864, 816 cm⁻¹.

Tranglimine 10

The title compound was obtained according to the published procedure.[1]

m.p. decomposed above 200 °C;

¹H NMR (300 MHz, CDCl₃): δ = 8.47 (d, *J* = 13.47, 1H), 8.07 (dd, *J* = 4.74, 14.16, 1H), 7.66 (m, 1H), 7.20 (m, 1H), 6.76 (m, 1H), 3.60 (m, 2H), 3.37 (m, 3H), 1.77 (m, 6H), 1.40 (m, 2H);

¹³C NMR (400 MHz, CDCl₃): δ = 160.56, 160.40, 160.33, 158.75, 158.71, 158.64, 158.61, 156.85, 156.78, 156.69, 156.66, 139.29, 139.25, 139.23, 127.15, 127.08, 127.04, 127.01, 126.95, 126.90, 126.86, 126.85, 123.32, 123.13, 122.94, 122.82, 107.21, 107.16, 107.03, 106.97, 77.04, 74.41, 74.33, 74.27, 74.10, 74.08, 73.64, 55.38, 55.37, 55.35, 55.24, 32.94, 32.85, 32.79, 32.76, 32.70, 32.62, 24.52;

MS (HR MALDI-TOF⁺): m/z found 727.4305 [M+H]⁺, calcd C₄₅H₅₅N₆O₆ 727.4257;

[α]_D²⁰ -239.6 (c = 1, CHCl₃);

IR (ATR): $\tilde{\nu}$ = 2926, 2855, 1633, 1606, 1569, 1450, 1413, 1383, 1344, 1303, 1260, 1194, 1159, 1034, 933, 865, 821, 752 cm⁻¹.

Trianglimine 11.

The title compound was obtained according to the previously published procedure.[5]

m.p. decomposed above 300 °C;

¹H NMR (300 MHz, CDCl₃): δ = 12.25 (s, 1H), 8.16 (s, 1H), 6.68 (s, 1H), 13.30 (m, 1H), 1.45 - 1.86 (m, 4H);

¹³C NMR (400 MHz, CDCl₃): δ = 163.92, 152.49, 121.00, 118.37, 73.82, 32.95, 24.17;

MS (HR ESI-TOF⁺): m/z found 733.3709 [M+H]⁺, calcd C₄₂H₄₉N₆O₆ 733.3714;

[α]_D²⁰ -407.1 (c = 1, CHCl₃);

IR (ATR): $\tilde{\nu}$ = 2928, 2700, 2858, 2653, 1622, 1510, 1448, 1362, 1310, 1216, 1158, 1098, 1041, 855, 811 cm⁻¹.

Trianglimine 12

The title compound was obtained according to the previously published procedure.[5]

m.p. decomposed above 280 °C;

¹H NMR (300 MHz, DMSO-*d*₆): δ = 12.40 (s, 1H), 8.63 (s, 1H), 7.11 - 7.31 (m, 5H), 6.89 (s, 1H), 5.10 (s, 1H);

¹³C NMR (400 MHz, DMSO-*d*₆): δ = 165.97, 152.25, 139.86, 128.81, 128.48, 127.98, 121.42, 118.93, 78.79;

MS (HR ESI-TOF⁺): m/z found 1027.4210 [M+H]⁺, calcd C₆₆H₅₅N₆O₆ 1027.4183;

[α]_D²⁰ -74.6 (c = 1, CHCl₃);

IR (ATR): $\tilde{\nu}$ = 3029, 2856, 1623, 1490, 1452, 1352, 1308, 1217, 1158, 1062, 1028, 753, 693, 581 cm⁻¹.

Trianglimine 13

The title compound was obtained according to published procedure.[4]

m.p. decomposed above 300 °C;

^1H NMR (300 MHz, CDCl_3): δ = 8.53 (s, 1H), 7.30 (s, 1H), 3.74 (s, 3H), 3.36 (m, 1H), 1.80 (m, 3H), 1.47 (m, 1H);

^{13}C NMR (400 MHz, CDCl_3): δ = 156.36, 152.94, 127.31, 109.61, 74.21, 56.00, 32.79, 24.51;

MS (HR ESI-TOF⁺): m/z found 817.4666 $[\text{M}+\text{H}]^+$, calcd $\text{C}_{48}\text{H}_{61}\text{N}_6\text{O}_6$ 817.4653;

$[\alpha]_{\text{D}}^{20}$ -241.5 (c = 1, CHCl_3);

IR (ATR): $\tilde{\nu}$ = 2927, 2855, 1630, 1489, 1463, 1408, 1384, 1284, 1209, 1156, 1042, 939, 879, 688 cm^{-1} .

Trianglimine *rac*-9

The solution of *rac*-1 (30 μL , 28.53 mg, 0.25 mmol), 2-hydroxyterephthalaldehyde (**4**, 37.5 mg, 0.25 mmol) and CHCl_3 (10 mL) was stirred under argon atmosphere at room temperature for 24h. After that time, the solvent was evaporated to obtain a yellow product with quantitatively yield. NMR spectra were identical as those measured for the optically pure **9**.

m.p. decomposed above 250 °C;

MS (HR ESI-TOF⁺): m/z found 685.3874 $[\text{M}+\text{H}]^+$, calcd for $\text{C}_{42}\text{H}_{49}\text{N}_6\text{O}_3$ 685.3866;

IR (ATR): $\tilde{\nu}$ = 2926, 2855, 2659, 1623, 1566, 1512, 1447, 1367, 1342, 1291, 1211, 1165, 1140, 1090, 1038, 973, 935, 864, 816, cm^{-1} .

Trianglimine *rac*-10

The solution of *rac*-1 (30 μL , 28.53 mg, 0.25 mmol), 2-methoxyterephthalaldehyde (**5**, 41 mg, 0.25 mmol) and CHCl_3 (10 mL) was stirred under argon atmosphere at room temperature for 24h. After that time, the solvent was evaporated and the crude product was recrystallized from EtOAc to obtain a white solid with quantitatively yield. NMR spectra were identical as those measured for the optically pure **10**.

m.p. does not melt to 300 °C;

MS (HR ESI-TOF⁺): m/z found 727.4349 $[\text{M}+\text{H}]^+$, calcd for $\text{C}_{45}\text{H}_{55}\text{N}_6\text{O}_3$ 727.4336;

IR (ATR): $\tilde{\nu}$ = 2926, 2855, 1633, 1606, 1569, 1450, 1413, 1383, 1344, 1303, 1260, 1194, 1159, 1119, 1086, 1034, 933, 865, 821, 752 cm^{-1} .

Trianglimine *rac*-11

The solution of *rac*-1 (33 μL , 31 mg, 0.27 mmol), 2,5-dihydroxyterephthalaldehyde (**6**, 45 mg, 0.27 mmol) and CHCl_3 (15 mL) was stirred under argon atmosphere at room temperature for 7 days. After that time, to the mixture was added EtOH (5 mL). The product was crystallized as yellow-orange solid with almost quantitatively yield. NMR spectra were identical as those measured for the optically pure **11**.

m.p. decomposed above 290 °C;

MS (HR MALDI-TOF⁺) : m/z found 733.3742 $[\text{M}+\text{H}]^+$, calcd for $\text{C}_{42}\text{H}_{49}\text{N}_6\text{O}_6$ 733.3714;

IR (ATR): $\tilde{\nu}$ = 2925, 2856, 2703, 2656, 1623, 1514, 1446.96, 1359, 1311, 1216, 1157, 1098, 1045, 939, 855, 811 cm^{-1} .

Trianglimine *rac*-12

The solution of *rac*-2 (127.8 mg, 0.6 mmol), 2,5-dihydroxyterephthalaldehyde (**6**, 100 mg, 0.6 mmol) and CHCl₃ (100 mL) was stirred under argon atmosphere at room temperature for 7 days. After that time, to the mixture was added EtOH (20 mL). The mixture of [2+2] and [3+3] products crystallized as yellow solid with 15:85 ratio with quantitatively total yield.

m.p. decomposed above 298 °C;

¹H NMR (300 MHz, CDCl₃): δ = 12.30 (s, 1H), *11.99 (s, 0.15H), 8.37 (s, 1H), *8.16 (s, 0.15H), 7.29 - 7.10 (m, 6.5H), 6.79 (s, 1H), *6.68 (s, 0.15H), 4.70 (s, 1H), *4.44 (s, 0.15H);

MS (HR ESI-TOF⁺): m/z found 1027.4198 [M+H]⁺, calcd C₆₆H₅₅N₆O₆ 1027.4183;

m/z found *685. 2822 [M+H]⁺, calcd C₄₄H₃₇N₄O₄ 685.2815;

IR (ATR): $\tilde{\nu}$ = 3030, 2859, 1621, 1491, 1453, 1353, 1309, 1217, 1158, 1087, 1063, 1029, 873, 800, 757, 692, 578 cm⁻¹.

Asterisks indicate signals originated from contracted [2+2] macrocycle.

Trianglimine *rac*-13

The solution of *rac*-1 (30 μL, 28.53 mg, 0.25 mmol), 2,5-dimethoxyterephthalaldehyde (**7**, 48.5 mg, 0.25 mmol) and CHCl₃ (10 mL) was stirred under argon atmosphere at room temperature for 24h. After that time, solvent was evaporated under reduced pressure and the crude product was recrystallized from EtOAc to obtain a white solid with almost quantitatively yield. NMR spectra were identical as those measured for the optically pure **13**.

m.p. decomposed above 300 °C;

MS (HR ESI-TOF⁺): m/z found 817.4666 [M+H]⁺, calcd C₄₈H₆₁N₆O₆ 817.4653;

IR (ATR): $\tilde{\nu}$ = 3362, 2924, 1855, 1629, 1489, 1463, 1407, 1383, 1345, 1285, 1206, 1157, 1091, 1042, 938, 901, 881, 854, 753, 732, 689 cm⁻¹.

Calculations details

The possible structures that include both constitutional and conformational isomers of imine macrocycles as well as model compounds were pre-optimized at the molecular mechanic level (MM3 force field as implemented in Scigress software).[6] Then all structures found at this stage were optimized at the B3LYP/6-31(d) level and re-optimized with the use of the same hybrid functional and enhanced triple- ζ basis set 6-311G(d,p). To estimate solvent influence on the structure and energies of the species under study, the IEFPCM solvent model of chloroform was employed.[7] The structures thus obtained were the real minimum energy isomers. The total and free energy values were used to obtain the Boltzmann population at 298.15 K.

Comments regarding plausible mechanism of trianglimine **9** formation

The intense peak of $m/z = 247$, visible in ESI-MS spectra shown in Figure S2b, corresponds to the protonated [1+1] monoimine **14**, which after condensation with another DACH molecules forms at first [1+2] and then [2+2] intermediates **15** and **16**, respectively. The peak of $m/z = 638$ corresponding to the complex of protonated [2+3] tetraimine **17** with methanol molecule is of the low intensity, which suggests that the process of the macrocycle-ring closing is very fast and is carried out after condensation with another DACH molecule.

DFT calculations have revealed that the stereochemical course of the reaction is determined at the stage of formation the [2+2] intermediate **15**. From the three structural types possible for this species, the one having the OH groups engaged in hydrogen bonding with the imine nitrogen atoms belonging to different diamine moieties, was the most abundant and covered 60% of the energetically allowed structures (see Table S1 and Figure S4). However, starting from this particular structural type, formation of either symmetrical or non-symmetrical final product **9** is equally possible. The remaining structural types covered the rest 40% of the energetically allowed structures, which are responsible for the formation of C1-symmetrical trianglimine **9**. In general, DFT calculations revealed a strong preference to the formation of the imine bond(s), stabilized by the intramolecular hydrogen bonds. For the simplest case of **14**, the calculated difference in the Gibbs free energy between two constitutional isomers reached 1 kcal mol⁻¹ in favor of the OH...N=C hydrogen bonded system (see Figure S4 and Table S1 in SI).

Details of SCXRD measurements

Single crystals suitable for X-ray analysis were obtained by slow evaporation from either ethanol (**9**, and solid solution of **8**, **18** and **19**) or chloroform (*rac*-**9**, **12**). All crystals were unstable in normal conditions, therefore for the purpose of X-ray analysis they were covered with the crystal protection grease and the diffraction data were collected at 130K. All investigated species displayed poor diffraction ability, and provided relatively low resolution data. Moreover, mixed crystals of **8**, **18** and **19** were twinned around [1 0 0] direct lattice direction. X-ray intensities were collected on the Oxford Diffraction SuperNova diffractometer equipped with Atlas CCD detector using mirror monochromatized Cu $K\alpha$ radiation ($\lambda = 1.54184 \text{ \AA}$).[8] Data reduction and analysis were carried out

with the CrysAlisPro program.[8] The structures were solved by direct methods with the SHELXT-2014 program and refined using full-matrix least-squares method with the SHELXL-2014 program.[9] All non-hydrogen atoms constituting a macrocycle were refined with anisotropic displacement parameters. In crystal structures of **9**, *rac*-**9** and **12** solvent molecules were localized and modelled for disorder. Non-H atoms constituting the major component of the disorder were refined anisotropically, while those belonging to the minor component were refined using an isotropic approximation. Hydrogen atoms bound to carbon atoms were placed in idealized positions and their coordinates refined using a riding model with isotropic displacement parameters equal to $1.2U_{eq}(C)$. The positions of the hydrogen atoms attached to the oxygen atoms were determined on the basis of the likely hydrogen bond scheme and refined as riding with $1.2U_{eq}(O)$. Interpretation of the results was performed using ORTEP software and Mercury program.[10] In cases where the Flack parameter appeared meaningless, the absolute structure of the crystals was assumed from the known absolute configuration of the reagents used in the synthesis.[11]

Crystal data and structure refinement details for **9**, *rac*-**9**, **12** and solid solution of **8**, **18** and **19** were collected in Table S2. CCDC 1821356 (**9**), 1821357 (*rac*-**9**), 1821358 (**12**) and 1821359 (solid solution of **8**, **18** and **19**) contain the supplementary crystallographic data for this paper. These data can be obtained free of charge from The Cambridge Crystallographic Data Centre via www.ccdc.cam.ac.uk/data%5Frequest/cif.

Table S1. Total energies (in Hartree) relative energies (ΔE , $\Delta\Delta G$, in kcal mol⁻¹) and percentage populations of model compounds A-F, calculated at the IEFPCM/B3LYP/6-311G(d,p) level of theory (for structures see Figure S3).

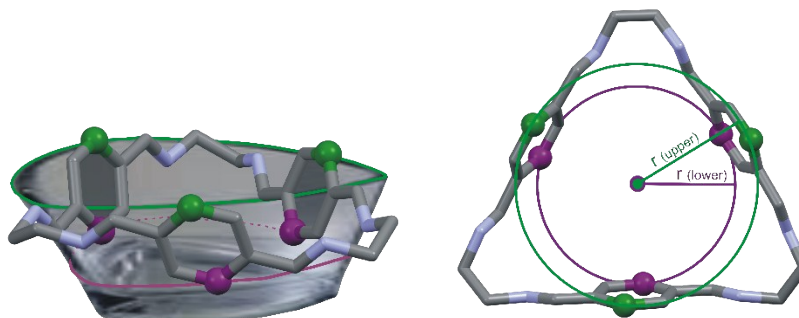
Compound	Energy	ΔE	Pop.	$\Delta\Delta G$	Pop.
A(1)	-749.131835	0.00	68.27	0.00	61.83
A(2)	-749.131112	0.45	31.73	0.29	38.17
A(3)	-749.129981	0.00	71.3	0.00	68.13
A(4)	-749.111069	11.87		10.74	
A(5)	-749.113635	10.26		8.94	
A(6)	-749.117228	8.00		7.05	
A(7)	-749.113997	10.03		8.81	
A(8)	-749.115773	8.92		7.83	
A(9)	-749.129122	0.54	28.7	0.45	31.87
A(10)	-749.112236	11.14		10.10	
14(1)	-804.496301	0.00	67.11	0.00	69.59
14(2)	-804.495627	0.42	32.89	0.49	30.41
14(3)	-804.49481	0.00	70.81	0.00	78.85
14(4)	-804.475935	11.84		11.28	
14(5)	-804.478507	10.23		9.30	
14(6)	-804.482064	8.00		7.43	
14(7)	-804.478802	10.05		8.90	
14(8)	-804.480551	8.95		8.17	
14(9)	-804.493974	0.52	29.19	0.78	21.15
14(10)	-804.477045	11.15		10.45	
B(1)	-1262.317177	0.23	19.55	0.58	14.76
B(2)	-1262.317549	0.00	29	0.00	39.46
B(3)	-1262.317177	0.23	19.55	0.58	14.78
B(4)	-1262.316698	0.53	11.76	0.56	15.24
B(5)	-1262.316254	0.81	7.35	1.13	5.83
B(6)	-1262.316048	0.94	5.91	1.07	6.53
B(7)	-1262.315848	1.07	4.78	1.45	3.41
B(8)	-1262.315075	1.55	2.11	2.39	
B(9)	-1262.314311	2.03		2.26	
B(10)	-1262.313949	2.26		2.74	
16(1)	-1532.540689	0.51	13.76	0.88	9.12
16(2)	-1532.540148	0.85	7.76	1.19	5.45
16(3)	-1532.53966	1.15	4.62	0.37	21.49
16(4)	-1532.541498	0.00	32.42	0.79	10.65
16(5)	-1532.540805	0.43	15.56	1.15	5.77
16(6)	-1532.541043	0.29	20.03	0.00	40.42
16(7)	-1532.538177	2.08		1.39	3.84
16(8)	-1532.539565	1.21	4.18	2.17	

16(9)	-1532.538696	1.76	1.67	2.31	
16(10)	-1532.538273	2.02		1.49	3.26
C(1)	-1802.763134	0.26	11.66	1.51	2.17
C(2)	-1802.762582	0.61	6.5	0.00	27.79
C(3)	-1802.762046	0.94	3.68	0.93	5.81
C(4)	-1802.763549	0.00	18.1	0.27	17.7
C(5)	-1802.76297	0.36	9.79	0.54	11.16
C(6)	-1802.763214	0.21	12.69	0.68	8.77
C(7)	-1802.762696	0.54	7.33	0.47	12.61
C(8)	-1802.763465	0.05	16.56	1.22	3.52
C(9)	-1802.762814	0.46	8.3	0.79	7.3
C(10)	-1802.762406	0.72	5.39	1.28	3.18
D(1)	-2260.587963	1.18	6.03	1.48	4.59
D(2)	-2260.588185	1.04	7.62	1.38	5.52
D(3)	-2260.587998	1.16	6.25	1.09	8.97
D(4)	-2260.589839	0.00	43.97	0.00	56.38
D(5)	-2260.589654	0.12	36.14	0.49	24.54

Table S2. Crystallographic data and refinement details for **9**, *rac*-**9**, **12** and solid solution of **8**, **18** and **19**.

	9	<i>rac</i> - 9	12	solid solution of 8 , 18 and 19
Crystal data				
Chemical formula	(C ₄₂ H ₄₈ N ₆ O ₃) ·0.5(C ₂ H ₆ O)	(C ₄₂ H ₄₈ N ₆ O ₃) ·0.4(CHCl ₃)	(C ₆₆ H ₅₆ N ₆ O ₆) ·2(CHCl ₃)	(C ₄₂ H ₄₈ N ₆ O ₃)
CCDC no.	1821356	1821357	1821358	1821359
<i>M_r</i>	707.89	732.61	1265.88	684.86
Crystal system	Monoclinic	Monoclinic	Orthorhombic	Triclinic
Space group	<i>C</i> 2	<i>P</i> 2 ₁ / <i>n</i>	<i>P</i> 2 ₁ 2 ₁ 2 ₁	<i>P</i> 1
<i>a</i> (Å)	31.3723 (17)	9.8047 (1)	6.0032 (1)	5.7811 (3)
<i>b</i> (Å)	5.5593 (5)	43.1344 (4)	30.9388 (3)	15.3719 (9)
<i>c</i> (Å)	23.8849 (14)	19.4077 (2)	33.6555 (2)	23.4378 (8)
α (°)	90	90	90	102.629 (4)
β (°)	101.048 (6)	92.935 (1)	90	90.481 (3)
γ (°)	90	90	90	95.883 (4)
<i>V</i> (Å ³)	4088.5 (5)	8197.13 (14)	6250.90 (13)	2020.72 (18)
<i>Z</i>	4	8	4	2
<i>D_x</i> (Mg m ⁻³)	1.150	1.187	1.345	1.126
μ (mm ⁻¹)	0.59	1.30	2.97	0.57
Crystal size (mm)	0.40 × 0.05 × 0.02	0.36 × 0.20 × 0.15	0.70 × 0.10 × 0.10	0.35 × 0.03 × 0.03
Data collection				
Radiation type	Cu K _α	Cu K _α	Cu K _α	Cu K _α
Diffractometer	SuperNova	SuperNova	SuperNova	SuperNova
Temperature (K)	130	130	130	130
Absorption correction	multi-scan	multi-scan	multi-scan	multi-scan
<i>T_{min}</i> , <i>T_{max}</i>	0.731, 1.000	0.802, 1.000	0.512, 1.000	0.884, 1.000
No. of measured, independent and observed	14477, 7110, 4718	124647, 14488, 14182	56821, 11033, 10710	19412, 19412, 13108
[<i>I</i> > 2σ (<i>I</i>)] reflections				
<i>R_{int}</i>	0.108	0.028	0.037	-
(sin θ/λ) _{max} (Å ⁻¹)	0.595	0.595	0.595	0.541
Refinement				
<i>R</i> [<i>F</i> ² > 2σ (<i>F</i> ²)], <i>wR</i> (<i>F</i> ²), <i>S</i>	0.103, 0.293, 1.01	0.058, 0.148, 1.07	0.047, 0.126, 1.05	0.068, 0.183, 0.99
No. of reflections	7110	14488	11033	19412
No. of parameters	521	1068	812	938
No. of restraints	17	171	54	13
Δρ _{max} , Δρ _{min} (e Å ⁻³)	0.39, -0.29	0.52, -0.51	0.49, -0.54	0.33, -0.28
Absolute structure parameter	0.3 (8)	-	0.007 (4)	0.3 (3)

Table S3. Method of calculation of the diameter of the upper and lower rims of the triangular bowl-like macrocycles and the respective values in Å. To describe the dimensions of the upper and lower rims of the bowl we have approximated them to the circles of the radius defined by the shortest distance from the center of a rim to one of the carbon atoms belonging to the corresponding upper or lower part of the macrocycle. The centroid of each ring has been defined by three non-substituted carbon atoms, marked in green (upper rim) and magenta (lower rim), from three different phenyl linkers, each positioned *trans* to the imine nitrogen.



Crystal	Value of the diameter of the upper rim [Å]	Value of the diameter of the lower rim [Å]
9	7.73	6.82
<i>rac</i> - 9	7.49	6.34
	7.60 (80%)	6.69 (80%)
	7.36 (20%)	6.88 (20%)
12	8.00	6.39
Solid solution of 8 , 18 , 19	7.75	6.78
	7.66	6.93
8 [12]	7.44	6.36
11 [13]	7.55	7.16
8·EtOAc [14]	7.56	6.71

Table S4. Selected hydrogen bond parameters for **9**.

<i>D</i> —H... <i>A</i>	<i>D</i> —H (Å)	H... <i>A</i> (Å)	<i>D</i> ... <i>A</i> (Å)	<i>D</i> —H... <i>A</i> (°)
Intramolecular				
O1—H1...N1	0.84	1.84	2.583 (10)	147
O1'—H1'...N2	0.84	1.78	2.58 (5)	158
O2—H2...N3	0.84	1.79	2.541 (10)	148
O2'—H2'...N4	0.84	1.75	2.523 (17)	151
O3—H3...N5	0.84	1.79	2.55 (2)	150
O3'—H3'...N6	0.84	1.79	2.541 (12)	147

Table S5. Selected hydrogen bond parameters for *rac-9*.

$D-H\cdots A$	$D-H$ (Å)	$H\cdots A$ (Å)	$D\cdots A$ (Å)	$D-H\cdots A$ (°)
Intramolecular				
O1A—H1A \cdots N1A	0.84	1.53	2.349 (6)	165
O1A'—H1A' \cdots N2A	0.84	1.80	2.575 (3)	152
O2A—H2A \cdots N3A	0.84	1.79	2.570 (8)	154
O2A'—H2A' \cdots N4A	0.84	1.77	2.532 (3)	150
O3A—H3A \cdots N5A	0.84	1.84	2.536 (12)	139
O3A'—H3A' \cdots N6A	0.84	1.83	2.583 (2)	148
O1B—H1B \cdots N1B	0.84	1.85	2.608 (3)	150
O1B'—H1B' \cdots N2B	0.84	1.76	2.535 (5)	152
O2B—H2B \cdots N3B	0.84	1.85	2.622 (4)	152
O2B'—H2B' \cdots N4B	0.84	1.81	2.595 (5)	154
O2C—H2C \cdots N3B	0.84	1.63	2.431 (7)	159
O3B—H3B \cdots N5B	0.84	1.83	2.591 (3)	150
O3B'—H3B' \cdots N6B	0.84	1.73	2.511 (6)	154
Intermolecular				
C10A—H10A \cdots O3B ⁱⁱⁱ	0.99	2.55	3.431 (3)	149
C21A—H21A \cdots O3B ^{iv}	0.95	2.55	3.467 (3)	162
C24A—H24B \cdots O2A ^v	0.99	2.36	3.033 (9)	125
C29A—H29A \cdots O1A ⁱ	0.95	2.28	3.195 (5)	160
C37A—H37A \cdots O1B ⁱ	1.00	2.49	3.120 (5)	121
C38A—H38A \cdots O2B ^{vi}	0.99	2.45	3.326 (5)	147
C38A—H38B \cdots O1B ⁱ	0.99	2.52	3.123 (5)	119
C08B—H08B \cdots O3B ⁱ	0.95	2.64	3.496 (5)	150
C35B—H35B \cdots O2B ⁱⁱ	0.95	2.24	3.086 (4)	148
C35B—H35B \cdots O2C ⁱⁱ	0.95	2.30	3.199 (8)	158
C41B—H41C \cdots N5A ⁱⁱ	0.99	2.69	3.648 (3)	162
C41B—H41C \cdots O3A ⁱⁱ	0.99	2.24	2.864 (10)	120

Symmetry code(s): (i) $x+1, y, z$; (ii) $x-1, y, z$; (iii) $x, y, z+1$; (iv) $x+1, y, z+1$; (v) $-x+2, -y+1, -z+2$; (vi) $x+1/2, -y+3/2, z+1/2$.

Table S6. Selected hydrogen bond parameters for **12**.

$D-H\cdots A$	$D-H$ (Å)	$H\cdots A$ (Å)	$D\cdots A$ (Å)	$D-H\cdots A$ (°)
Intramolecular				
O1—H1 \cdots N1	0.84	1.83	2.569 (4)	146
O2—H2 \cdots N2	0.84	1.86	2.607 (4)	147
O3—H3 \cdots N3	0.84	1.82	2.571 (4)	148
O4—H4 \cdots N4	0.84	1.87	2.609 (5)	147
O5—H5 \cdots N5	0.84	1.90	2.642 (4)	146
O6—H6 \cdots N6	0.84	1.85	2.594 (4)	147
Intermolecular				
C04—H04 \cdots O2 ⁱ	0.95	2.66	3.385 (5)	134
C14—H14 \cdots O4 ⁱ	0.95	2.60	3.298 (6)	130
C17—H17 \cdots O3 ⁱⁱ	0.95	2.58	3.283 (5)	131

Symmetry code(s): (i) $x-1, y, z$; (ii) $x+1, y, z$.

Table S7. Selected hydrogen bond parameters for solid solution of **8**, **18** and **19**.

<i>D</i> —H... <i>A</i>	<i>D</i> —H (Å)	H... <i>A</i> (Å)	<i>D</i> ... <i>A</i> (Å)	<i>D</i> —H... <i>A</i> (°)
Intramolecular				
O1A—H1A...N1A	0.84	1.90	2.636 (10)	146
O2A—H2A...N2A	0.84	1.87	2.611 (10)	147
O3A—H3A...N3A	0.84	1.82	2.525 (12)	141
O4A—H4A...N4A	0.84	1.89	2.614 (13)	143
O1B—H1B...N1B	0.84	1.87	2.610 (10)	146
O2B—H2B...N2B	0.84	1.84	2.567 (11)	143
O3B—H3B...N3B	0.84	1.90	2.628 (11)	145
O4B—H4B...N4B	0.84	1.87	2.620 (11)	147
Intermolecular				
O2A—H2A...O3A ⁱ	0.84	2.49	2.770 (12)	101
O3B—H3B...O2B ⁱⁱ	0.84	2.29	2.687 (12)	109
C15A—H15A...O3A ⁱ	0.95	2.66	3.352 (13)	130
C23A—H23A...O4A ⁱⁱ	1.00	2.65	3.348 (14)	127
C41A—H41B...O4B ⁱⁱⁱ	0.99	2.57	3.470 (13)	152
C08B—H08B...O2B ⁱⁱ	0.95	2.60	3.320 (12)	133
C09B—H09B...O2B ⁱⁱ	1.00	2.64	3.458 (12)	139
C42B—H42B...O1B ⁱ	1.00	2.64	3.326 (12)	126

Symmetry code(s): (i) $x-1, y, z$; (ii) $x+1, y, z$; (iii) $x, y, z-1$.

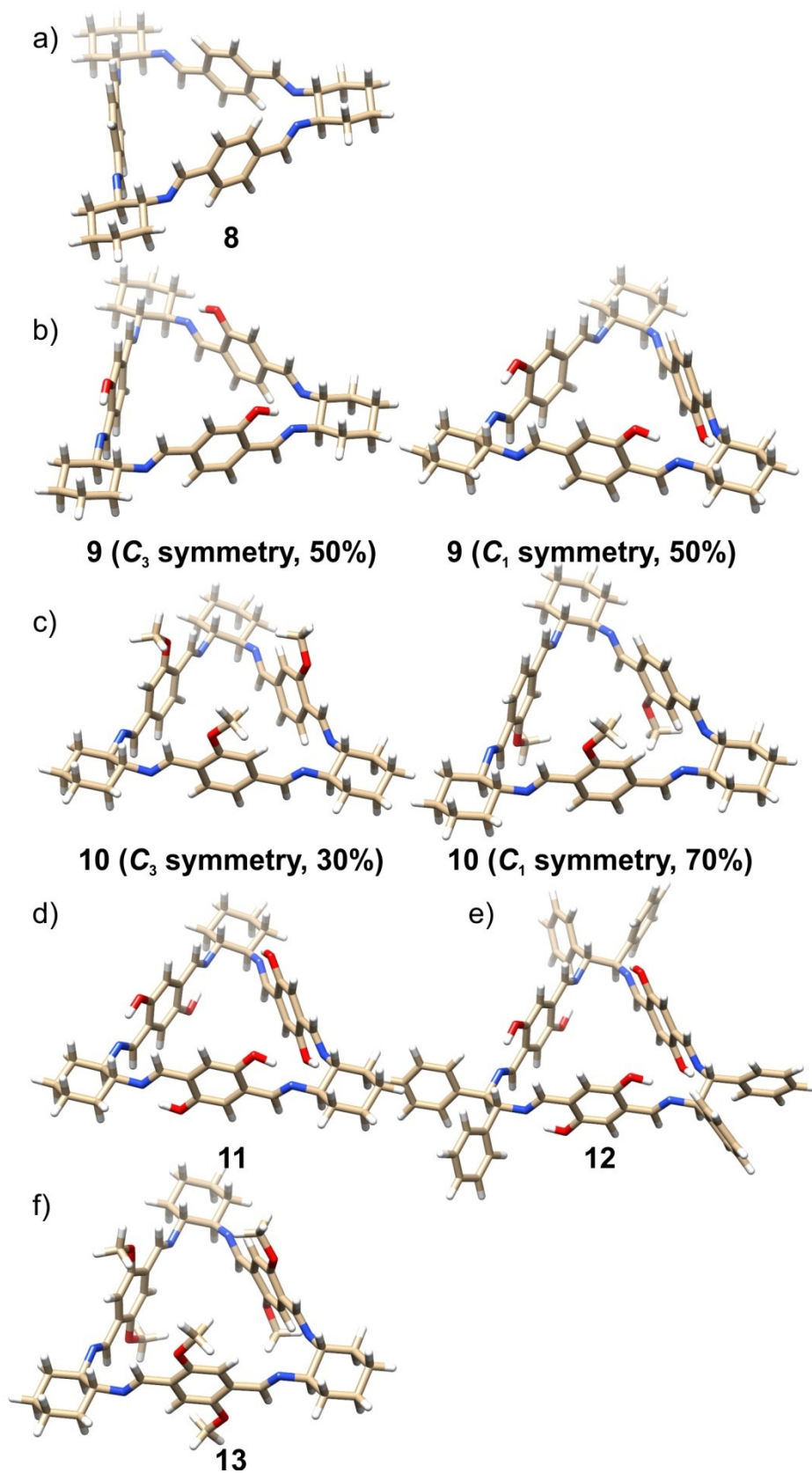


Figure S1. Calculated at the IEFPCM/B3LYP/6-311G(d,p) level low-energy structures of trianglimines **8-13**. Percentage quantities in parentheses refer to the $\Delta\Delta G^\circ$ -based populations.

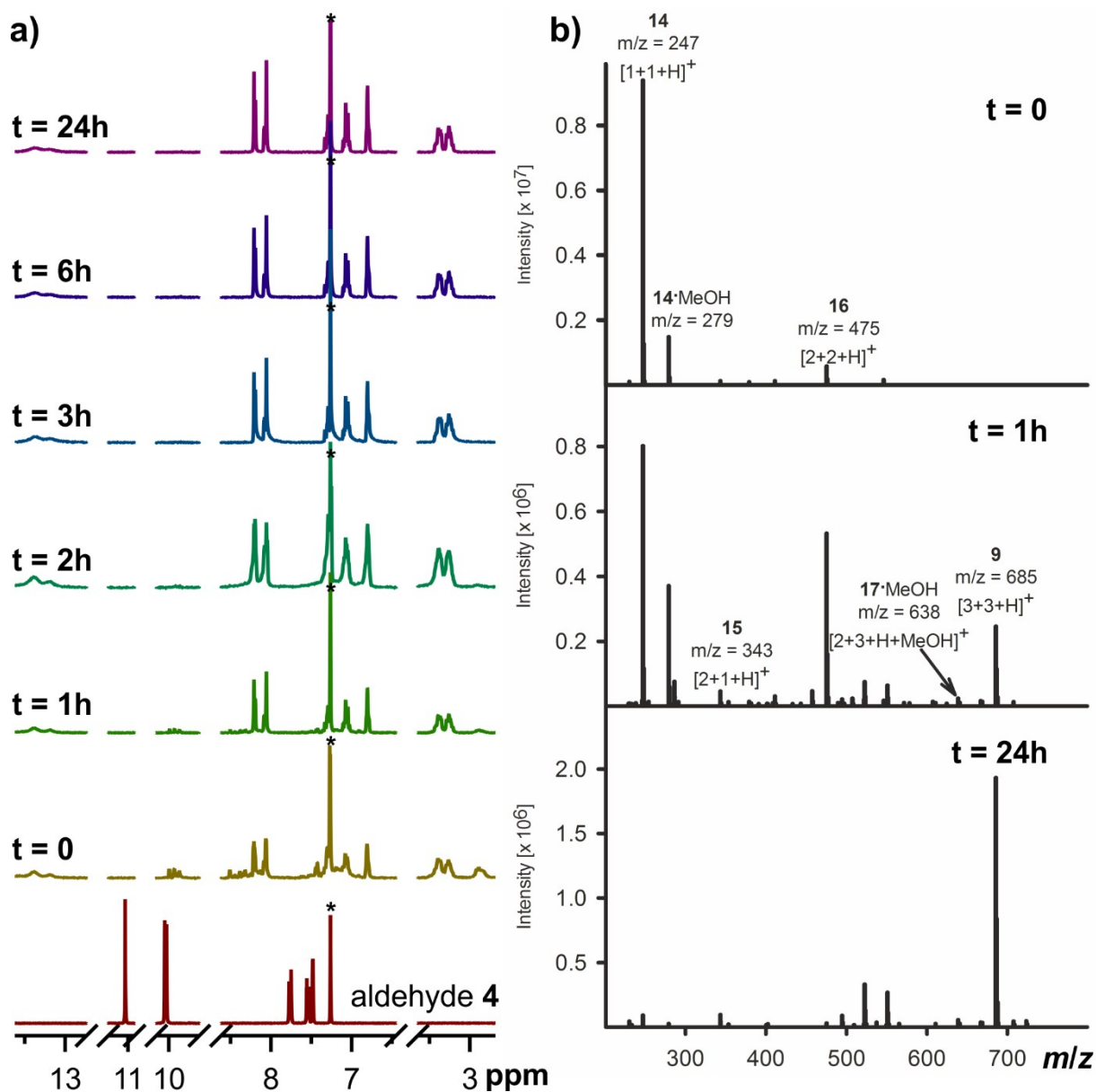


Figure S2. a) Diagnostic parts of the ^1H NMR spectra [CDCl₃, 300 MHz] measured during cycloimination reaction between (*R,R*)-**1** and **4**. At the bottom of column is shown diagnostic part of the ^1H NMR spectra of aldehyde **4**. Asterisks indicate trace solvent peaks. b) The exemplary ESI-MS spectra measured during cycloimination reaction between (*R,R*)-**1** and **4**.

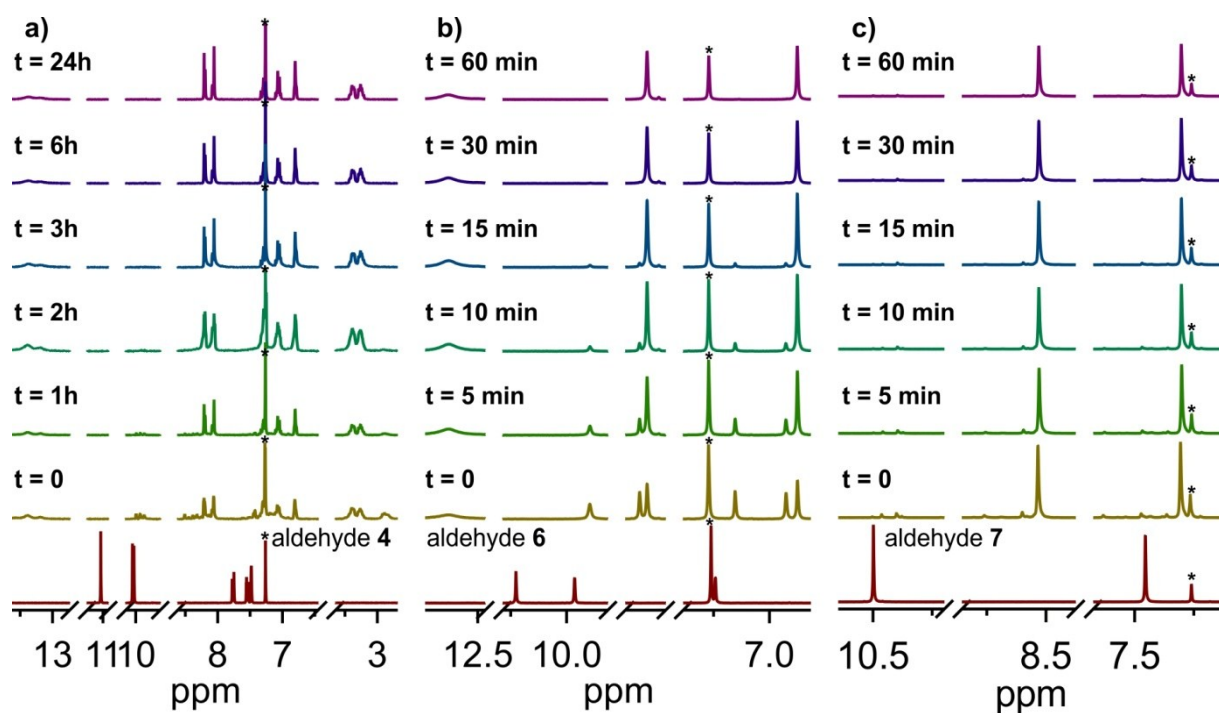
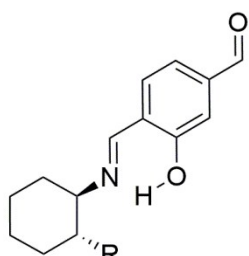
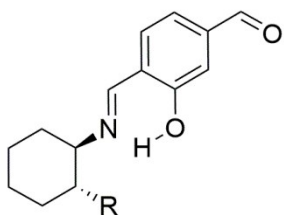


Figure S3. Diagnostic parts of the ^1H NMR spectra [CDCl_3 , 300 MHz] measured during cycloimination reaction between: a) (R,R) -**1** and **4**, b) (R,R) -**1** and **6**; a) (R,R) -**1** and **7**. At the bottom of each column is shown diagnostic part of the ^1H NMR spectra of the respective aldehyde. Asterisks indicate trace solvent peaks.

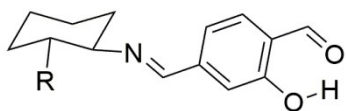


(1)

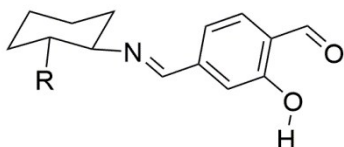


(2)

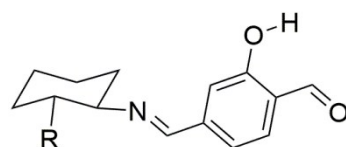
A, R = H
14, R = NH₂



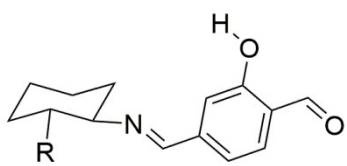
(3)



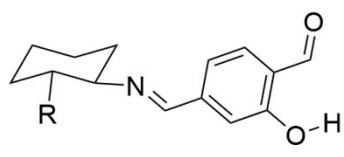
(4)



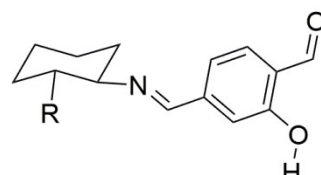
(5)



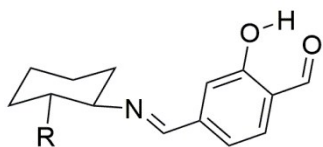
(6)



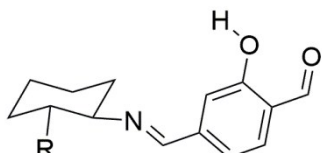
(7)



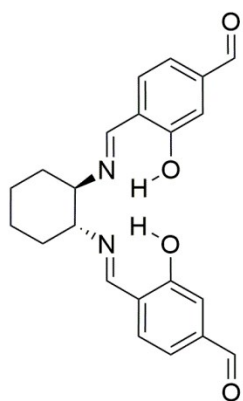
(8)



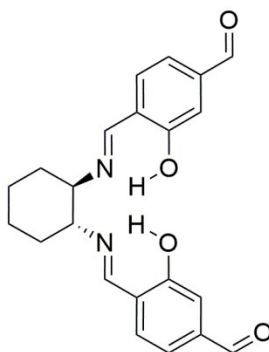
(9)



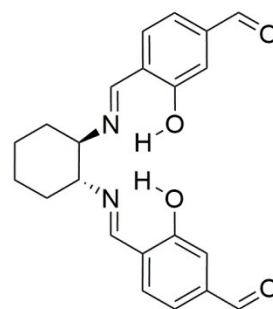
(10)



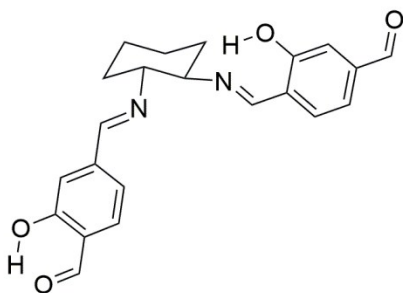
B(1)



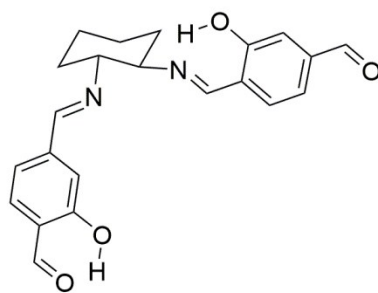
B(2)



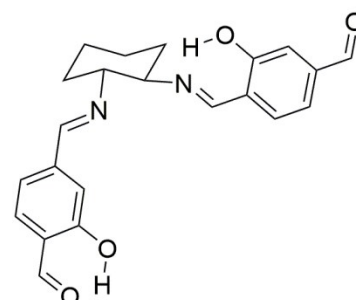
B(3)



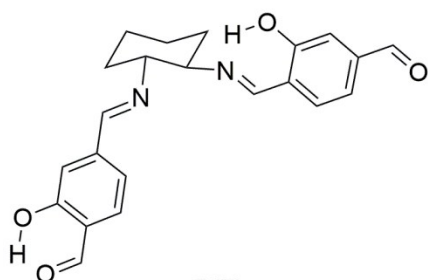
B(4)



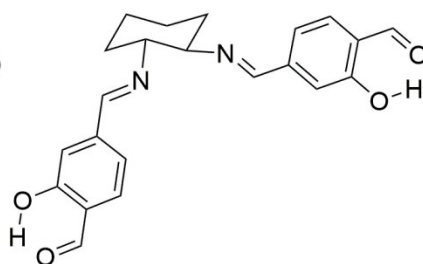
B(5)



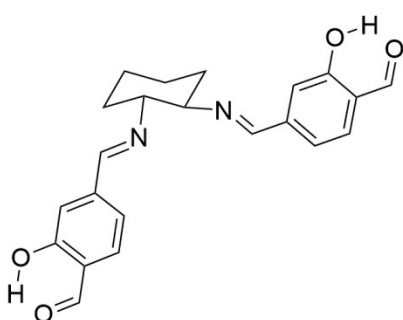
B(6)



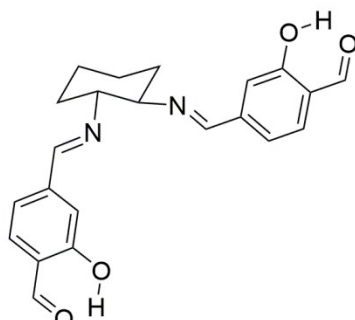
B(7)



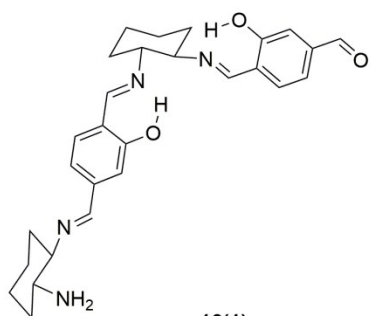
B(8)



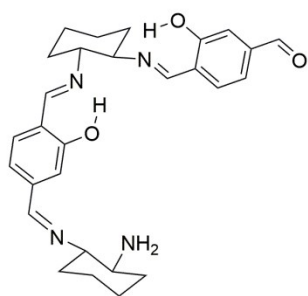
B(9)



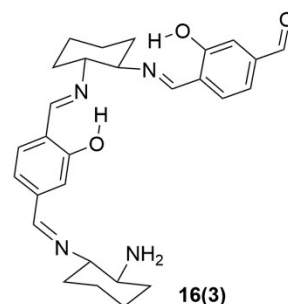
B(10)



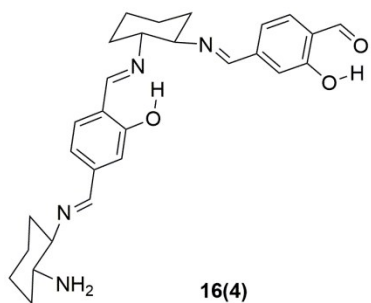
16(1)



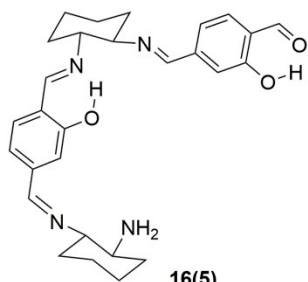
16(2)



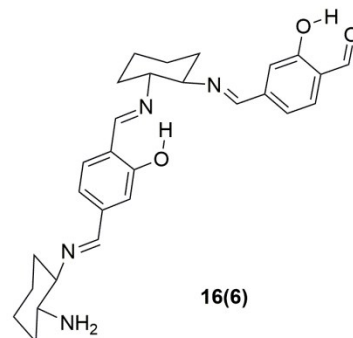
16(3)



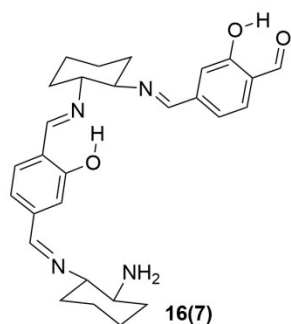
16(4)



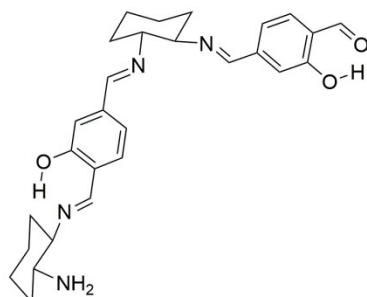
16(5)



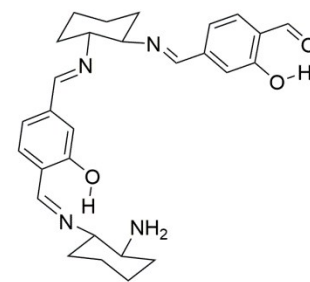
16(6)



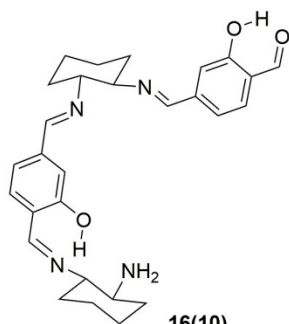
16(7)



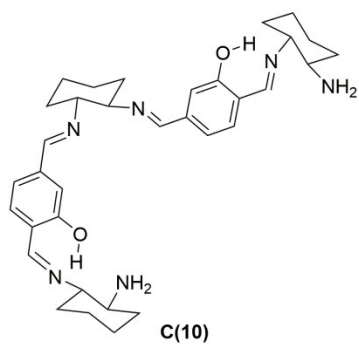
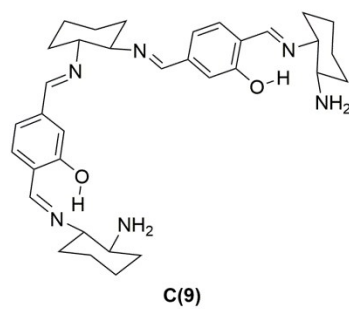
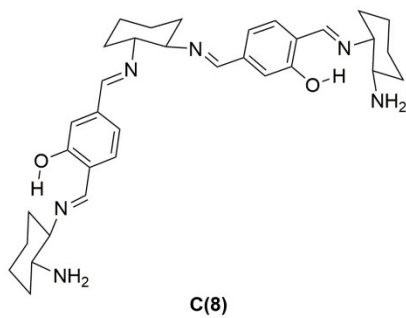
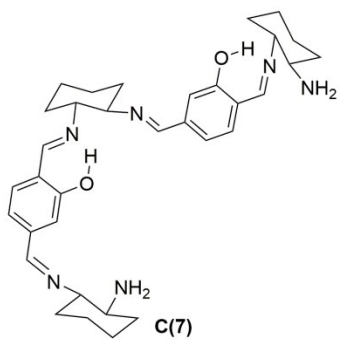
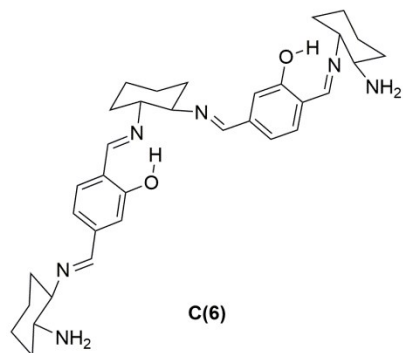
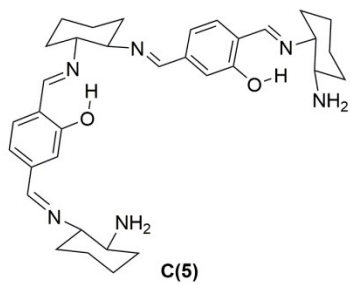
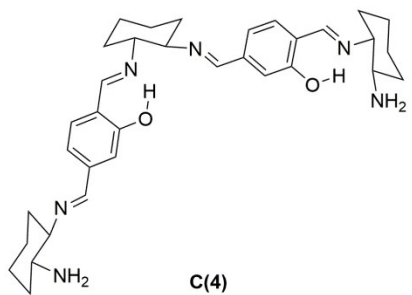
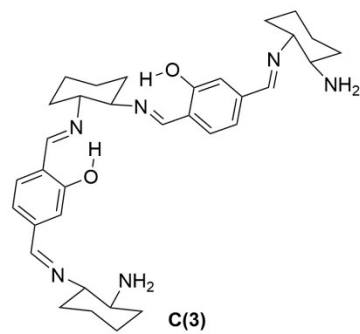
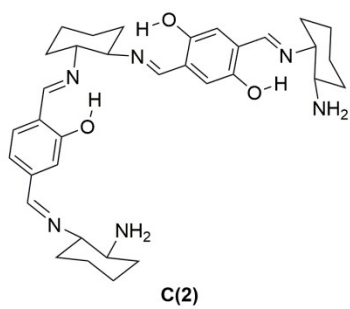
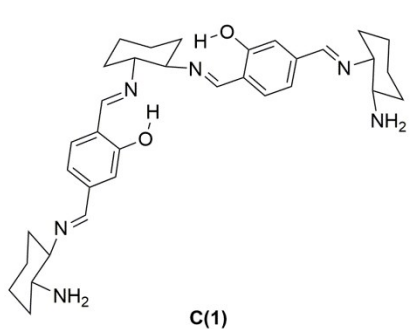
16(8)



16(9)



16(10)



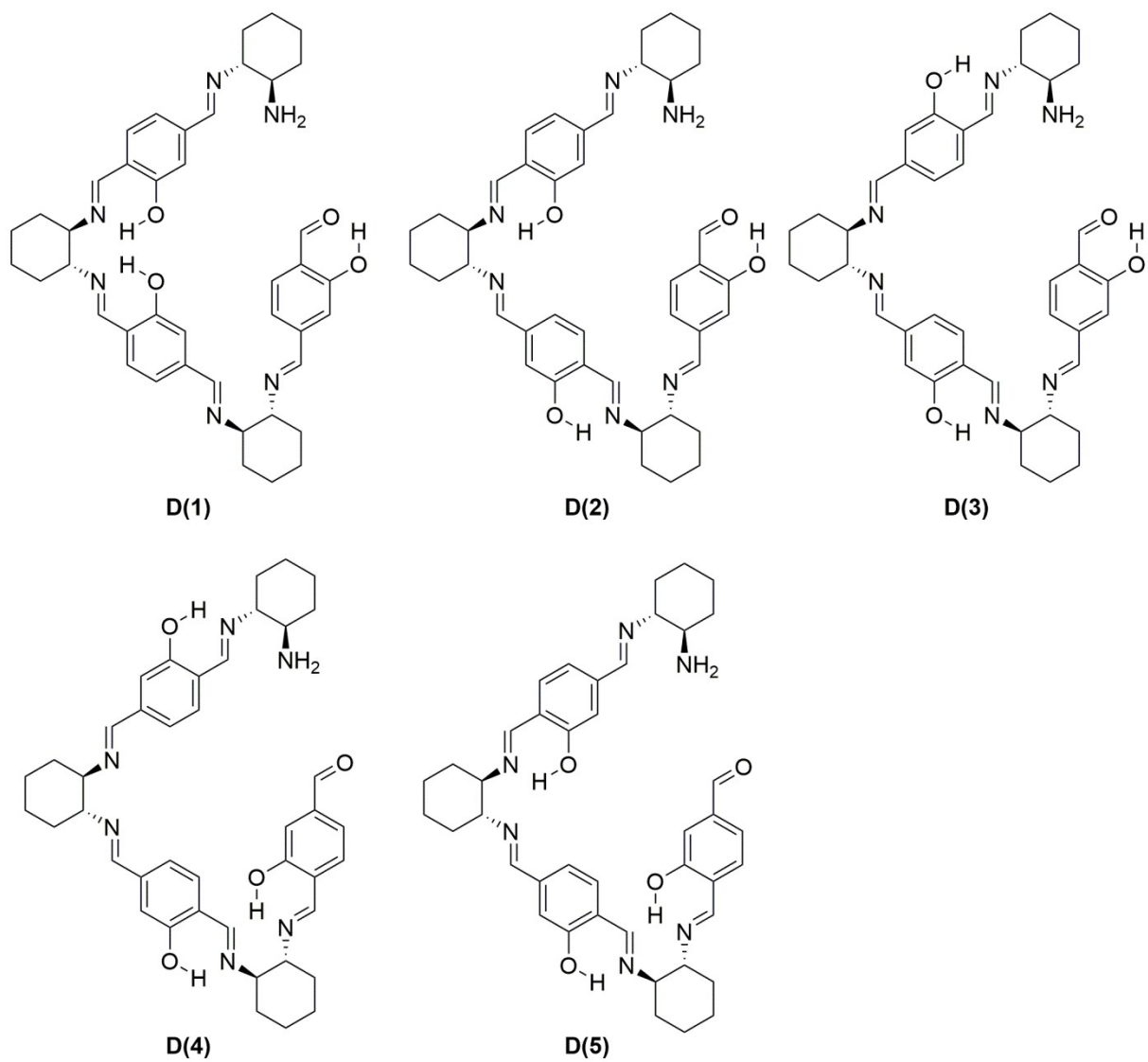


Figure S4. Structures of model compounds A-D, 14 and 16, calculated at the IEFPCM/B3LYP/6-311G(d,p) level of theory.

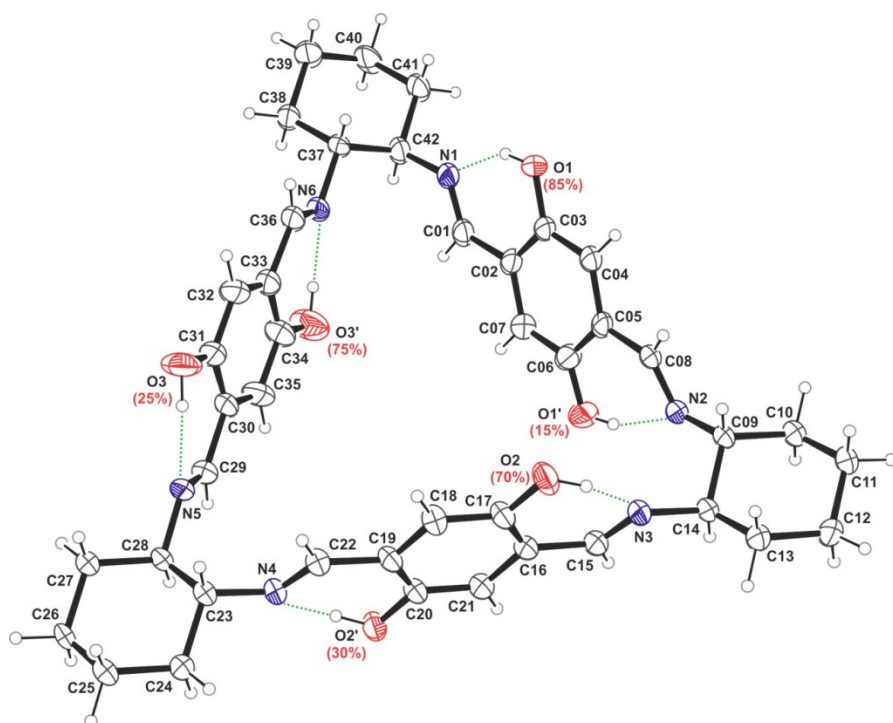


Figure S5. Structure of macrocyclic molecule **9** at 130K. Displacement ellipsoids are drawn at the 30% probability level. Hydrogen atoms are represented in arbitrary radii. Intramolecular hydrogen bonds (NH...O) are marked as green dashed lines. Values in parentheses represent the site occupation factors for the hydroxyl groups expressed as percentages. Compound **9** crystallizes in monoclinic system in $C2$ space group with 4 macrocyclic molecules and 2 molecules of ethanol in unit cell.

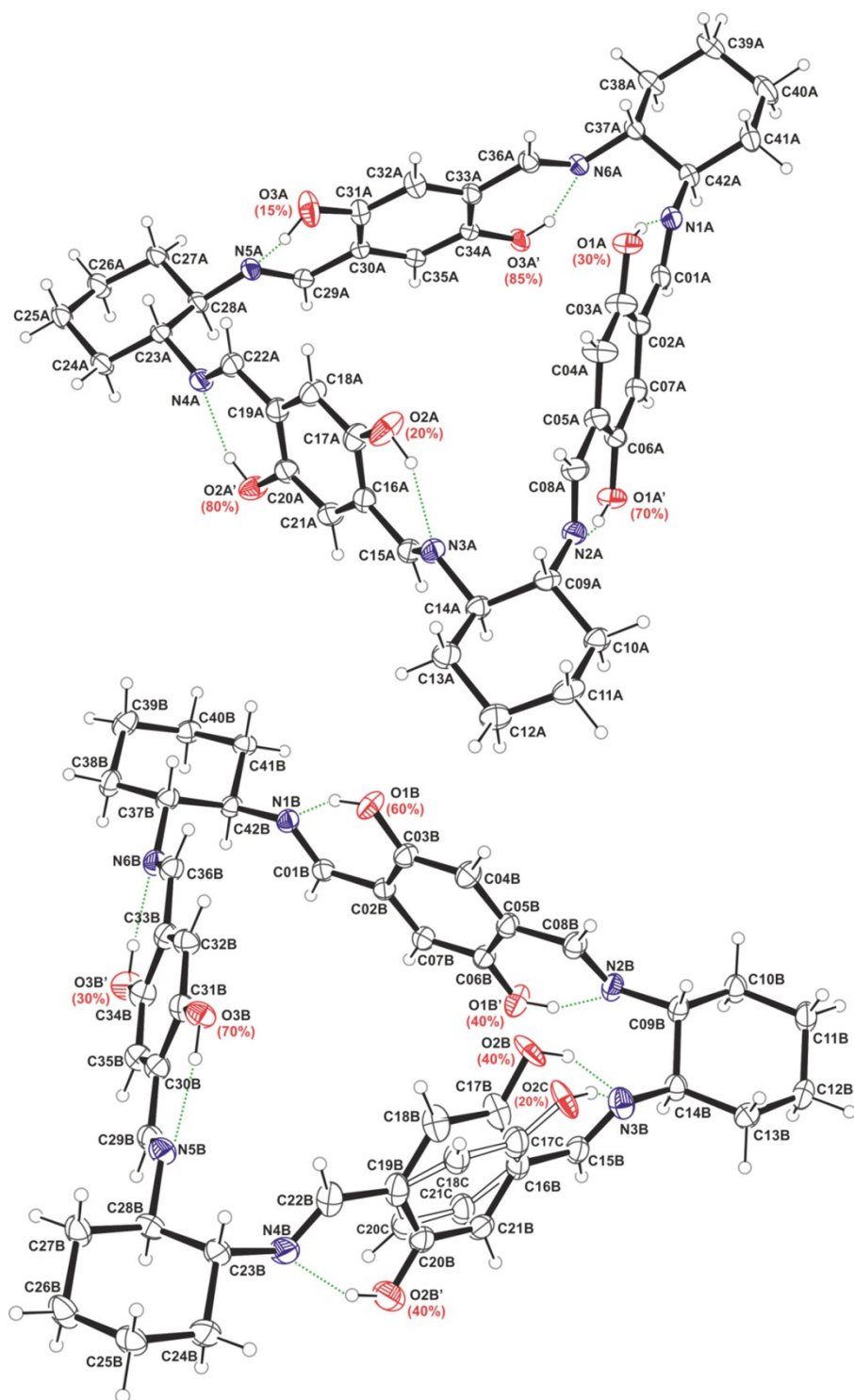


Figure S6. Structure of two symmetry independent macrocyclic molecules *rac-9*. Displacement ellipsoids are drawn at the 30% probability level. Hydrogen atoms are represented in arbitrary radii. Intramolecular hydrogen bonds (NH \cdots O) are marked as green dashed lines. Values in parentheses represent the site occupation factors for the hydroxyl groups expressed as percentages. Open bonds illustrate the second component of disorder within one of the aromatic spacers. *rac-9* crystallizes in $P2_1/n$ space group of the monoclinic system, with 8 macrocyclic molecules and 3.2 molecules of chloroform in the unit cell.

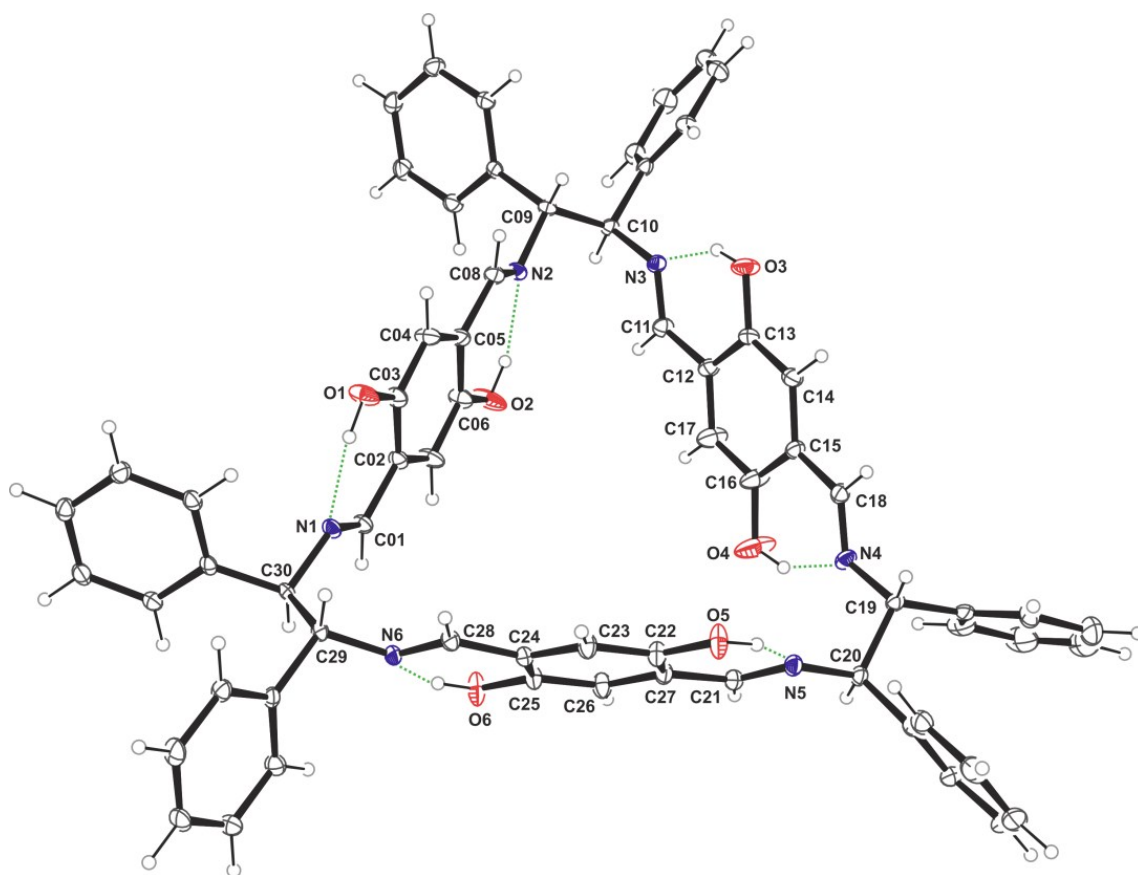


Figure S7. Structure of macrocyclic molecule **12**. Displacement ellipsoids are drawn at the 30% probability level. Hydrogen atoms are represented in arbitrary radii. Intramolecular hydrogen bonds (NH...O) are marked as green dashed lines. Compound **12** crystallizes in orthorhombic system in $P2_12_12_1$ space group with 4 macrocyclic molecules and 8 molecules of chloroform in unit cell.

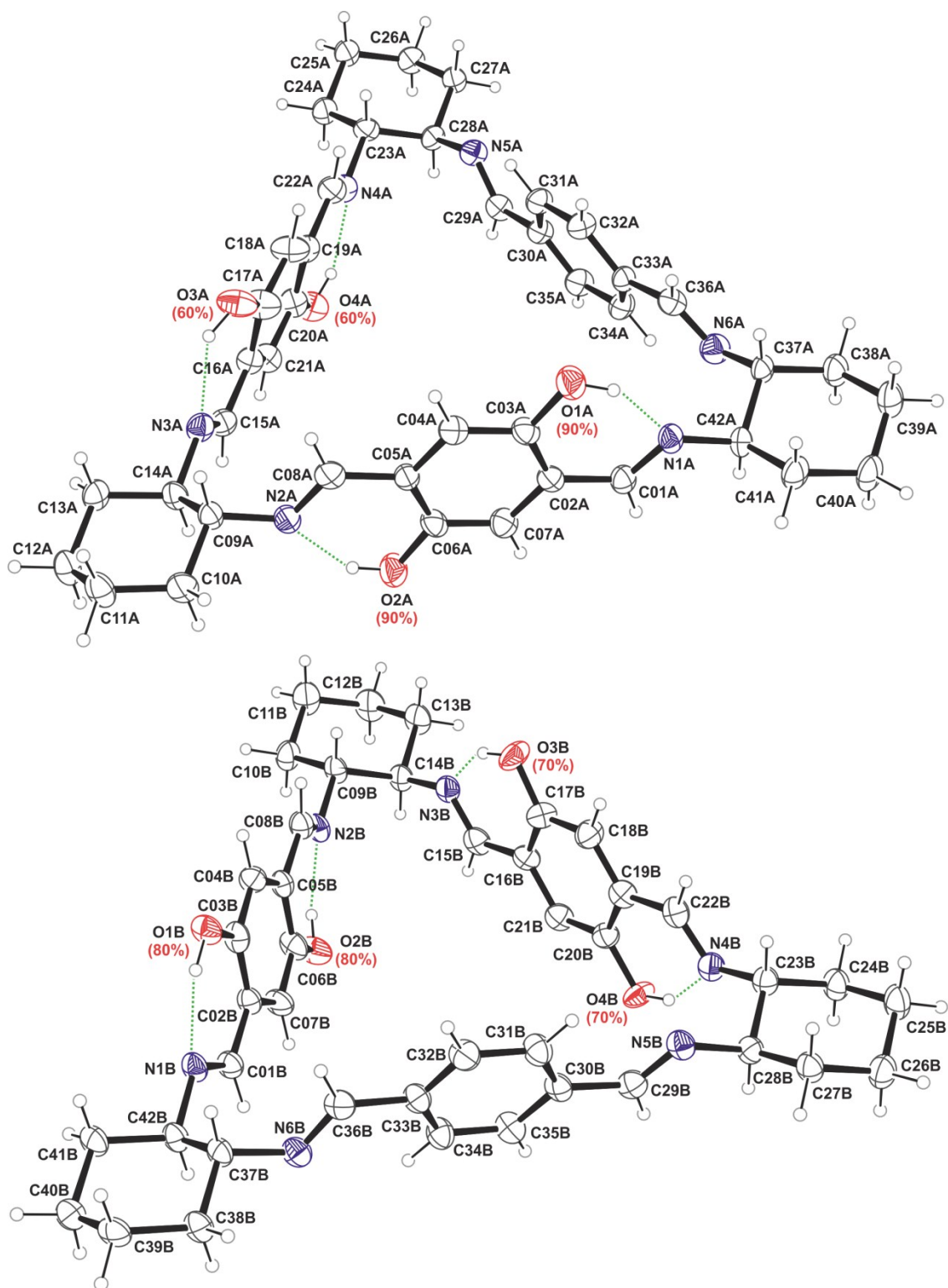


Figure S8. Structure of two symmetry independent ‘averaged’ macrocyclic molecules of solid solution of **8**, **18** and **19**. Displacement ellipsoids are drawn at the 30% probability level. Hydrogen atoms are represented in arbitrary radii. Intramolecular hydrogen bonds are marked as green dashed lines. Values in parentheses represent the site occupation factors for the hydroxyl groups expressed as percentages. The unit cell of triclinic *P1* symmetry contains two nearly identical ‘averaged’ molecules

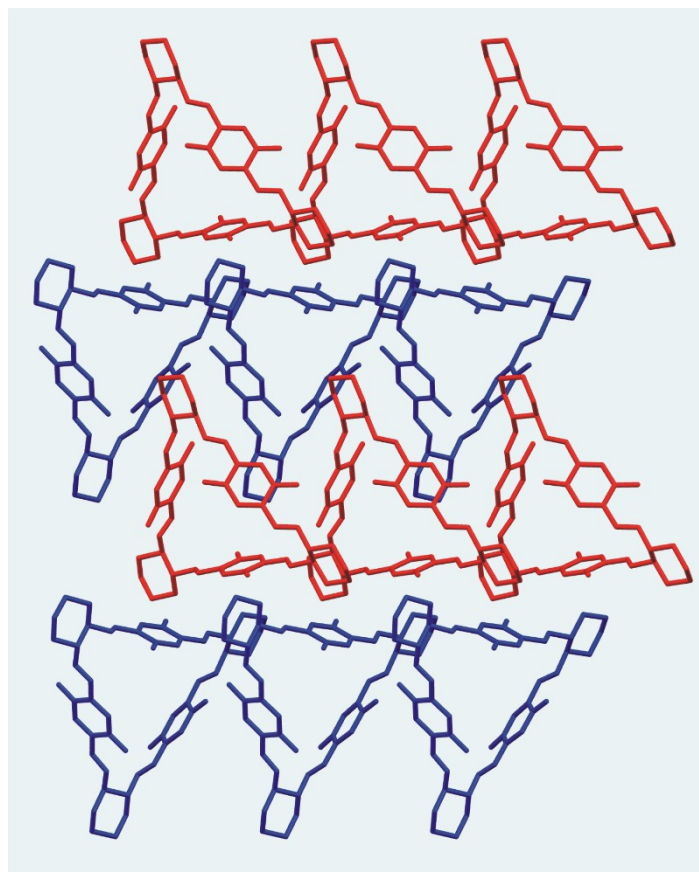


Figure S9. View of one of the chiral layers formed in the crystals of *rac*-**9**. The layer contains solely all-*(R)* enantiomers. Two independent 'averaged molecules' are distinguished by deep-blue and red colours. Hydrogen atoms and chloroform solvent molecules have been omitted.

References

- [1] J. Gajewy, J. Szymkowiak, M. Kwit; *RSC Adv.*, 2016, **6**, 53358.
- [2] Y. Okada, M. Sugai, K. Chiba, Kazuhiro; *J. Org. Chem.*, 2016, **81**, 10922.
- [3] N. Kuhnert, G. M. Rossignolo, A. Lopez-Periago; *Org. Biomol. Chem.*, 2003, **1**, 1157.
- [4] J. Gawroński, K. Gawrońska, J. Grajewski, M. Kwit, A. Plutecka, U. Rychlewska; *Chem. Eur. J.*, 2006, **12**, 1807.
- [5] J. Szymkowiak, M. Kwit; *Chirality*, 2018, **30**, 117.
- [6] Scigress 2.5, Fujitsu Ltd.
- [7] M. J. Frisch, G. W. Trucks, H. B. Schlegel, G. E. Scuseria, M. A. Robb, J. R. Cheeseman, G. Scalmani, V. Barone, B. Mennucci, G. A. Petersson, H. Nakatsuji, M. Caricato, X. Li, H. P. Hratchian, A. F. Izmaylov, J. Bloino, G. Zheng, J. L. Sonnenberg, M. Hada, M. Ehara, K. Toyota, R. Fukuda, J. Hasegawa, M. Ishida, T. Nakajima, Y. Honda, O. Kitao, H. Nakai, T. Vreven, J. A. Montgomery Jr., J. E. Peralta, F. Ogliaro, M. Bearpark, J. J. Heyd, E. Brothers, K. N. Kudin, V. N. Staroverov, R. Kobayashi, J. Normand, K. Raghavachari, A. Rendell, J. C. Burant, S. S. Iyengar, J. Tomasi, M. Cossi, N. Rega, N. J. Millam, M. Klene, J. E. Knox, J. B. Cross, V. Bakken, C. Adamo, J. Jaramillo, R. Gomperts, R. E. Stratmann, O. Yazyev, A. J. Austin, R. Cammi, C. Pomelli, J. W. Ochterski, R. L. Martin, K. Morokuma, V. G. Zakrzewski, G. A. Voth, P. Salvador, J. J. Dannenberg, S. Dapprich, A. D. Daniels, Ö. Farkas, J. B. Foresman, J. V. Ortiz and J. Cioslowski, D. J. Fox, Gaussian 09, revision A.02, Gaussian, Inc., Wallingford CT, 2009.
- [8] CrysAlis PRO 1.171.38.43, Rigaku Oxford Diffraction, 2015.
- [9] a) G. M. Sheldrick; *Acta Cryst. A*, 2015, **71**, 3; b) G. M. Sheldrick; *Acta Cryst. C*, 2015, **71**, 3.
- [10] a) ORTEP-3 for Windows; L. J. Farrugia, *J. Appl. Cryst.*, 2012, **45**, 849; b) Mercury - Crystal Structure Visualisation, Version 3.9; C. F. Macrae, P. R. Edgington, P. McCabe, E. Pidcock, G. P. Shields, R. Taylor, M. Towler and J. van de Streek; *J. Appl. Cryst.*, 2006, **39**, 453.
- [11] H. D. Flack; *Acta Cryst. A*, 1983, **39**, 876; S. Parsons, H. D. Flack, T. Wagner; *Acta Cryst. B*, 2013, **69**, 249.
- [12] M. Chadim, M. Buděšínský, J. Hodačová, J. Závada, P. C. Junk; *Tetrahedron: Asym.*, 2001, **12**, 127.
- [13] S. Srimurugan, B. Viswanathan, T. K. Varadarajan, B. Varghese; *Tetrahedron Lett.*, 2005, **46**, 3151.
- [14] J. Gawroński, H. Kolbon, M. Kwit, A. Katrusiak; *J. Org. Chem.*, 2000, **65**, 5768.